Validation and Application of Altimetry-Derived Upper Ocean Thermal Structure in the Western North Pacific Ocean for Typhoon-Intensity Forecast

Iam-Fei Pun, I-I Lin, Chau-Ron Wu, Dong-Shan Ko, and W. Timothy Liu

***Abstract*—This paper uses more than 5000 colocated and near-coincident *in-situ* profiles from the National Oceanic and Atmospheric Administration/Global Temperature and Salinity Profile Program database spanning over the period from 2002 to 2005 to systematically validate the satellite-altimetry-derived upper ocean thermal structure in the western North Pacific ocean as such ocean thermal structure information is critical in typhoon-intensity change. It is found that this satellite-derived information is applicable in the central and the southwestern North Pacific (covering 122–170° E, 9–25° N) but not in the northern part (130–170° E, 25–40° N). However, since $> 80\%$ of the typhoons are found to intensify in the central and southern part, this regional dependence should not pose a serious constraint in studying typhoon intensification. Further comparison with the U.S. Naval Research Laboratory's North Pacific Ocean Nowcast/Forecast System (NPACNFS) hydrodynamic ocean model shows similar regional applicability, but NPACNFS is found to have a general underestimation in the upper ocean thermal structure and causes a large underestimation of the tropical cyclone heat potential (TCHP) by up to 60 kJ/cm^2. After validation, the derived upper ocean thermal profiles are used to study the intensity change of supertyphoon Dianmu (2004). It is found that two upper ocean parameters, i.e., a typhoon's self-induced cooling and the during-typhoon TCHP, are the most sensitive parameters (with $R^2 \sim 0.7$) to the 6-h intensity change of Dianmu during the study period covering Dianmu's rapid intensification to category 5 and its subsequent decay to category 4. This paper suggests the usefulness of satellite-based upper ocean thermal information in future research and operation that is related to typhoon-intensity change in the western North Pacific.**

***Index Terms*—Altimetry, typhoon, upper ocean thermal structure.**

I. Introduction

THE WESTERN North Pacific is among the world oceans where most tropical cyclones occur. Here, an average of 30 cyclones (including tropical storms, depressions, and typhoons from category 1 to 5[1]) are found each year. In comparison, $\leqq 20$ cyclones are found in the Eastern Pacific and the Atlantic, while $\leqq 10$ cyclones are found in the Southern Pacific Ocean each year. In the western North Pacific, cyclones profoundly impact the half-billion people living near the Asian coasts. This can be clearly demonstrated in the case of recent Supertyphoon Saomai (August 2006) in which eastern China was devastated with a death toll of 300 and a loss of 1.5 billion USD.

Although with such impact, the current typhoon-intensity-forecast skill in the western North Pacific still has much room for improvement. Unlike the situation in the Atlantic where coupled hurricane–ocean models are used in the operational forecast [1], here, most of the operational models remain uncoupled and use only the prescribed sea-surface temperature (SST) to represent the ocean's role in the forecast. As pointed out by Bender and Ginis [1], Emanuel [3], Emanuel *et al.* [4], and Shay *et al.* [32], this is not realistic because cyclones interact not only with the surface but also with the entire upper ocean column (typically down to 200 m). In the uncoupled/prescribed-SST forecast, the ocean's dynamic response due to the cyclone's wind forcing is not included; thus, the critical negative feedback due to the cyclone's self-induced cooling is not considered and can lead to considerable error in intensity forecast

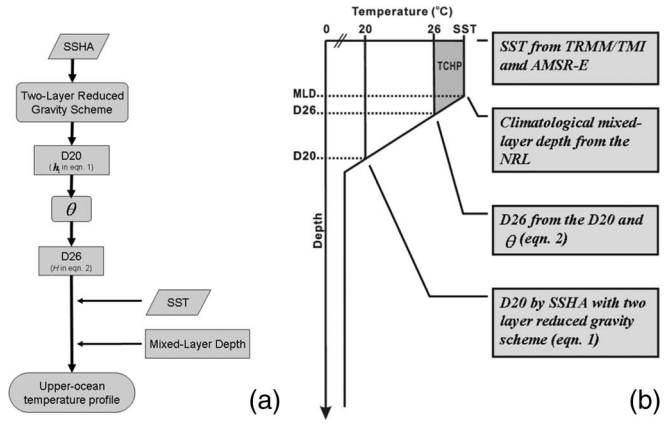

Fig. 1. (a) Flowchart showing the steps that are involved in the TLM_WNP. (b) Schematic diagram illustrating the TLM_WNP method in retrieving upper ocean thermal profile.

Manuscript received May 1, 2006; revised October 30, 2006. This work was supported in part by Grants NSC 95-2611-M-002-024-MY3, NSC 95-2119-M-002-040-AP1, and NSC 96-2111-M-002-001.

I.-F. Pun and I-I Lin (corresponding author) are with the Department of Atmospheric Sciences, National Taiwan University, Taipei 106, Taiwan, R.O.C. (e-mail: faye@webmail.as.ntu.edu.tw; iilin@webmail.as.ntu.edu.tw).

C.-R. Wu is with the Department of Earth Sciences, National Taiwan Normal University, Taipei 106, Taiwan, R.O.C. (e-mail: cwu@cc.ntnu.edu.tw).

D.-S. Ko is with the Coastal and Semi-Enclosed Sea Section, Naval Research Laboratory, Stennis Space Center, MS 39529 USA (e-mail: ko@nrlssc.navy.mil).

W. T. Liu is with the Jet Propulsion Laboratory, California Institute of Technology, Pasadena, CA 91125 USA (e-mail: W.Timothy.Liu@jpl.nasa.gov).

Color versions of one or more of the figures in this paper are available online at http://ieeexplore.ieee.org.

Digital Object Identifier 10.1109/TGRS.2007.895950

[1]The Saffir–Simpson Tropical Cyclone Scale based on a 1-min average sustained wind speed (tropical depression: < 34 kn, tropical storm: 34–63 kn, category 1: 64–82 kn, category 2: 83–95 kn, category 3: 96–113 kn, category 4: 114–135 kn, and category 5: > 135 kn).

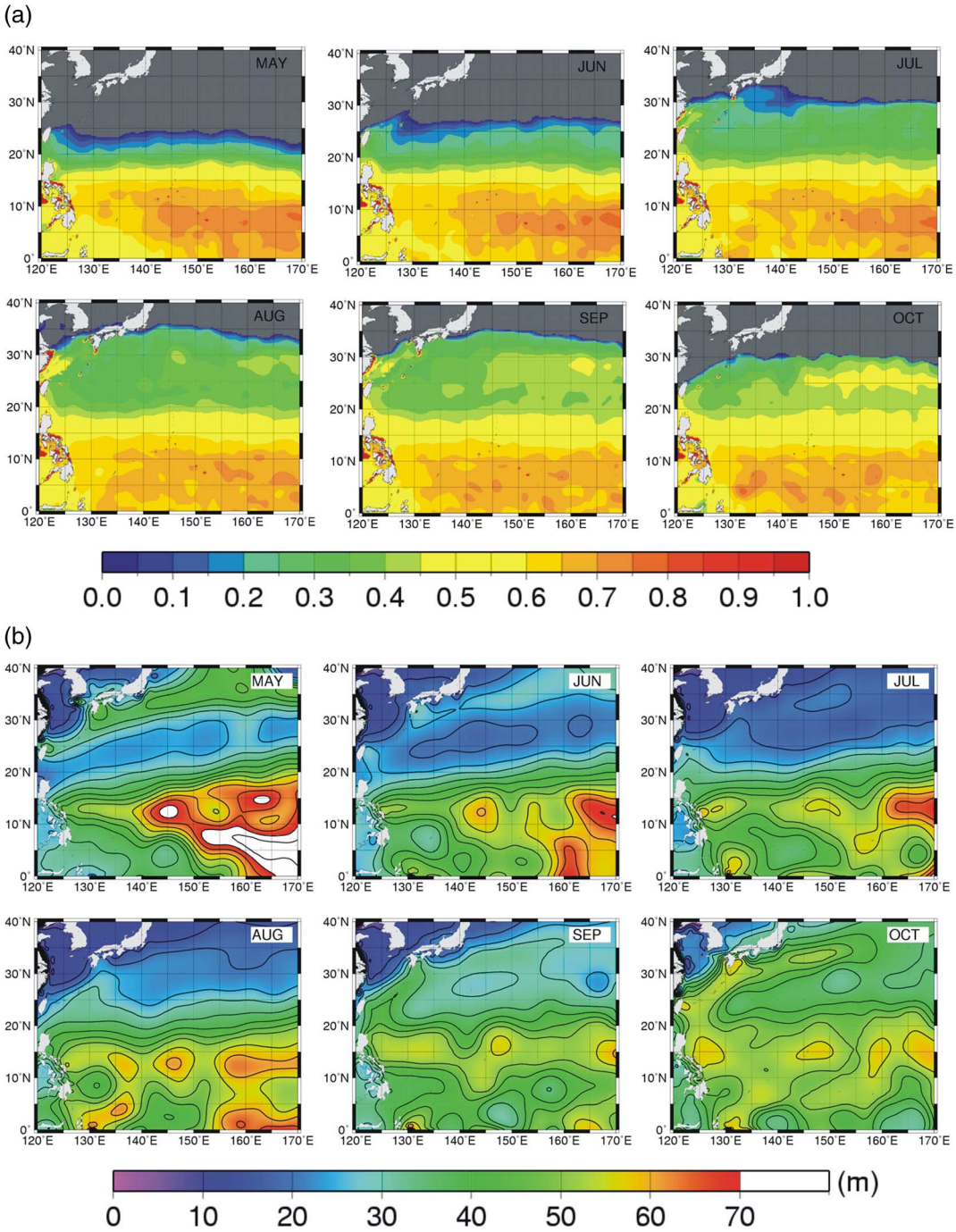

Fig. 2. (a) Monthly climatological ratio between D26 and D20 during May–October in the western North Pacific (Data source: NOAA/NODC/WOA01, [33]). Gray represents land or areas where the SST is lower than the 26 °C and no ratio can be calculated. (b) Monthly climatological mixed-layer depth from the U.S. NRL.

[1], [3], [4], [13]. To include the ocean's dynamic response in the forecast, one important prerequisite is to operationally obtain the upper ocean thermal structure information [1], [4], [20], [31], [35]. However, how to obtain such information over the vast western North Pacific ocean is a big problem since it is impossible to use *in-situ* measurements to meet this operational need. The satellite remote-sensing-based method thus becomes vital. It has been proposed by Goni *et al.* [9] and Shay *et al.* [32] that by using satellite altimetry and SST data as input to a simple two-layer reduced-gravity ocean model, one can obtain a first-order approximation of the upper ocean thermal information. This method has the advantage of fast calculation and simple implementation; thus, it is suitable for the operational needs and is currently adopted by the National Oceanic and Atmospheric Administration (NOAA) to operationally provide upper ocean thermal information over global oceans [10].

Clearly, it is necessary to validate this derived information so as to assess its applicability regionally. Since there is little such information for the western North Pacific region, this paper aims to conduct systematic validation using a large set (> 5000)

of coincident/colocated sea truth data from the NOAA/Global Temperature and Salinity Profile Program (GTSPP, [17]) during 2002–2005 to contribute to this need. Because this is a relatively simple model, additional comparison with a 26-sigma-level operational ocean model (the North Pacific Ocean Nowcast/Forecast System (NPACNFS) from the U.S. Naval Research Laboratory (NRL) [18]) is made. After validation, we use the derived upper ocean thermal structure information to study the intensity change of the most rapidly intensified (from category 1 to 5 in 18 h) western North Pacific typhoon since 1960, i.e., supertyphoon Dianmu (2004).

II. Upper Ocean Thermal Structure That Is Derived From the Two-Layer Method and Tropical Cyclone Heat Potential (TCHP)

Fig. 1(a) summarizes the steps that are involved to estimate the upper ocean thermal structure information using satellite altimetry and SST data in a two-layer reduced-gravity ocean model, as proposed by Goni *et al.* [9] and Shay *et al.* [32]. In the two-layer scheme, the ocean is separated into two layers of fluid. The 20 °C isotherm (which usually lies at the center of the main thermocline in most tropical regions [10], [32]) serves as a border that separates the upper and lower layers. The distance from the sea surface to the 20 °C isotherm (D20) is thus defined as the upper ocean thickness h_1. As the variations in the depth of the main thermocline (here defined as D20 or h_1) are associated with the variations in the sea-surface height. Thus, h_1 (or D20) can be estimated from the observed altimetry sea-surface height anomaly (SSHA or η') data as follows [9]:

$$h_1(x,y,t) = \overline{h_1}(x,y) + \frac{\rho_2(x,y)}{\rho_2(x,y) - \rho_1(x,y)}\eta'(x,y,t) \quad (1)$$

where $\overline{h_1}$ is the mean climatological upper layer thickness (i.e., the climatological D20), and ρ_1 and ρ_2 are the density of the upper (sea surface to 20 °C isotherm) and lower (20 °C isotherm to ocean bottom) layers, respectively. In this paper, the SSHA data are from the Jet Propulsion Laboratory's delayed mode data from the TOPEX/Poseidon and Jason-1 satellite altimeters [7]. With this product, SSHA is based on the difference between the observed sea-surface height and the six-year (1993–1998) mean of the sea-surface height data from multiple-altimetry missions including TOPEX/Poseidon, ERS-1, ERS-2, and GEOSAT [24]. $\overline{h_1}$ is from the high-resolution (25 × 25 km) climatological temperature data, i.e., the WOA01 data set (based on the *in-situ* data during 1982–2001) of the NOAA/National Ocean Data Center (NODC) [33]. ρ_1 and ρ_2 are also calculated from the WOA01 temperature and salinity database [22], [34]. Clearly, all parameters are functions of location (x, y) and time (t), except the climatological parameters (i.e., $\overline{h_1}$ and ρ), which are only functions of location (x, y). After estimation of the initial D20, the depth of the 26 °C isotherm (D26) is estimated based on the climatological ratio between D20 and D26 for each 1/4° by 1/4° grid point in the western North Pacific (domain: 120–170° E, 9–40° N) as

$$H(x,y,t) = \theta(x,y)h_1(x,y,t) \quad (2)$$

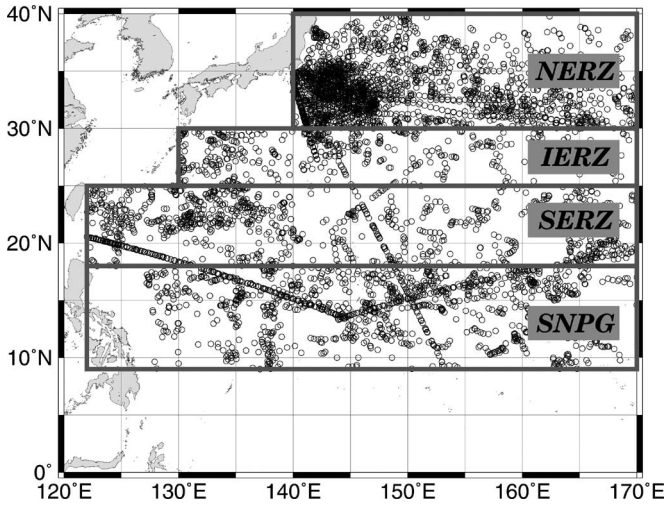

Fig. 3. Locations of the four validation zones in the western North Pacific including the SNPG, the SERZ, the NERZ, and the IERZ. Circles denote the locations of the 5684 GTSPP *in-situ* profiles that were used in the validation.

TABLE I
Number of Monthly *In-Situ* GTSPP Profiles That Are Used in Validation in Different Zones During 2002–2005

	SNPG	*SERZ*	*IERZ*	*NERZ*
May	238	134	70	31
June	254	222	113	294
July	225	218	100	530
August	245	235	132	568
September	141	171	178	607
October	195	171	166	446
Total	1298	1151	759	2476

where H represents D26, and θ is the climatological ratio that is also calculated from the WOA01 temperature database [33]. From [10] and [32], it is important to estimate the 26 °C isotherm because 26 °C represents a threshold temperature for tropical cyclone genesis and is commonly used in tropical cyclone research [6], [23]. The θ maps for each month during the May–October western North Pacific typhoon season are shown in Fig. 2(a).

Next, SST (Fig. 1) can be obtained directly from the cloud-penetrating Tropical Rainfall Measuring Mission/Microwave Imager (TRMM/TMI) and the Advanced Microwave Sounding Radiometer for the Earth Observing System (AMSR-E) [36]. Finally, the mixed-layer depth is obtained from the monthly averaged climatological mixed-layer depth data from the U.S. NRL [16] [Fig. 2(b)]. Thus, the upper ocean depth-temperature profile can be produced operationally to a first order at 1/4° (∼25 km) spatial resolution in a daily basis [Fig. 1(b)] [9], [10], [32]. It is referred to as TLM_WNP (Two-Layer Method for the Western North Pacific) hereafter in this paper.

After obtaining the upper ocean depth-temperature profile, TCHP can be calculated. TCHP was originally proposed by Leipper and Volgenau in 1972 as the integrated heat content from the depth of 26 °C isotherm to the surface. Recent works by Goni and Trinanes [10] and Shay *et al.* [32] report that as TCHP carries the information of the upper ocean thermal structure, it can provide useful information in studying the

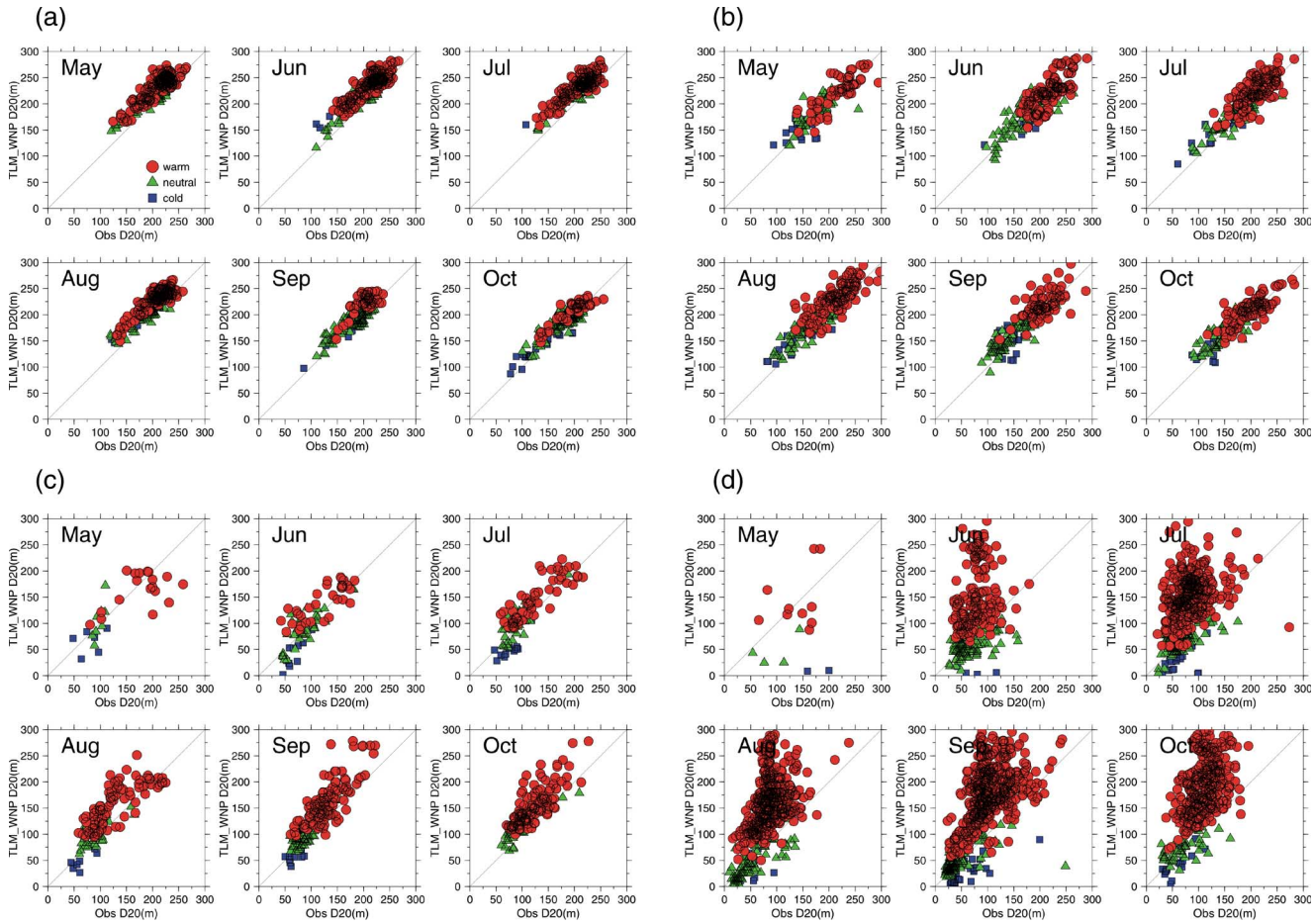

Fig. 4. Monthly scatter plots of the TLM_WNP-estimated D20 and the *in-situ* GTSPP D20 in the (a) SNPG, (b) SERZ, (c) IERZ, and (d) NERZ during 2002–2005. The matching pairs are separated into three groups representing warm feature pairs (SSHA $>$ 8 cm, red circles), neutral pairs (SSHA between -8 and 8 cm, green triangles), and cold feature pairs (SSHA < -8 cm, blue squares).

cyclone's intensity change. They proposed that, after obtaining the upper ocean thermal structure from the two-layer method, TCHP Q_H [10], [19], [32] can be calculated as

$$Q_H(x, y, t) = c_p \rho \Delta T(x, y, z, t) \Delta Z \tag{3}$$

where c_p is the capacity heat of the water at constant pressure, which is taken as 4178 J $\cdot$ kg^{-1} °C^{-1}; ρ is the average density of the upper ocean, which is taken as 1026 kg $\cdot$ m^{-3}; and ΔT is the difference between $T(z)$ and 26 °C over depth interval ΔZ. Clearly, Q_H is also a function of location (x, y) and time (t).

III. Validation of the Two-Layer-Method-Estimated Upper Ocean Thermal Structure by *In-Situ* Profiles

In this paper, 5684 colocated and near-coincident (acquired on the same day) *in-situ* temperature profiles from the NOAA/GTSPP [17] covering the May–October typhoon season from 2002 to 2005 are used for validation. Due to distinct hydrographical settings in the western North Pacific [14], [27], [30], [37], validation is done according to the four zones in the western North Pacific. These four zones are the Southern North Pacific Gyre (SNPG; 122–170° E, 9–18° N); two known eddy-rich zones, i.e., the South Eddy-Rich Zone (SERZ; 122–170° E, 18–25° N) and the North Eddy-Rich Zone (NERZ; 140–170° E, 30–40° N) [14], [20], [27], [30], [37]; and lastly, the Intermediate zone between the two Eddy-Rich Zones (IERZ; 130–170° E, 25–30° N). The locations of these four zones, together with the locations of the *in-situ* profiles, are shown in Fig. 3. The distribution of the location of these profiles over these zones during the typhoon season is given in Table I. The validation is done for the TLM_WNP D20, D26, and SST. For each month at each zone, the root mean square (rms) difference (which represents the absolute difference), the Percentage of RMS in the Observed Mean (PROM, which represents the difference of the estimated values relative to the observation), and bias are calculated.

A. Validation of the Depth of the 20° C Isotherm (D20)

D20 is the first parameter that is estimated from the two-layer algorithm (Section II) and is used to derive the 26 °C isotherm (D26). It is thus fundamental to assess the accuracy of D20 first since incorrect D20 will lead to subsequent incorrect estimation of D26. The monthly scatter plots comparing the derived and *in-situ* D20 during 2002–2005 are given in Fig. 4. In addition, in Fig. 4, the matching pairs are separated into three groups

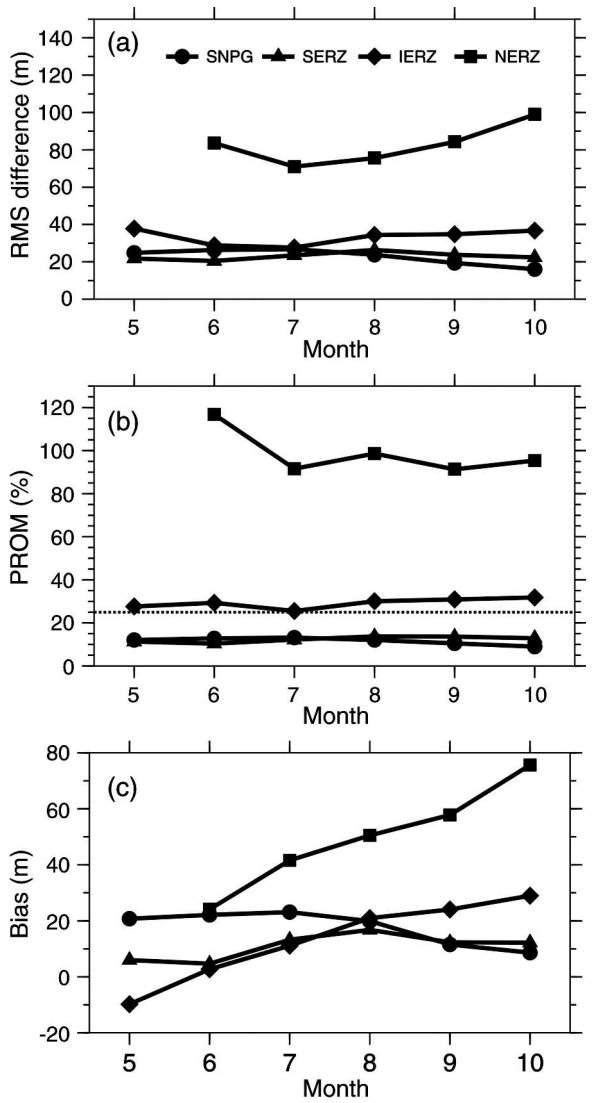

Fig. 5. (a) Monthly rms difference, (b) PROM, and (c) bias of the TLM_WNP-estimated D20 in each zone. The dotted line in (b) depicts the accuracy threshold of 25% PROM.

representing positive SSHA pairs (SSHA > 8 cm, corresponding to large values of D20), neutral pairs (SSHA between -8 and 8 cm), and negative SSHA pairs (SSHA < -8 cm, corresponding to small values of D20) [27]. The monthly accuracy analysis, in rms difference, bias, and PROM, are given in Fig. 5. As in May, there are very few matching data points (22 pairs) in the NERZ that can be used for validation because the water temperature was still cold and mostly below 20 °C and thus are not discussed. From Fig. 4, one can see that throughout May–October in the SNPG [Fig. 4(a)] and SERZ [Fig. 4(b)], the derived TLM_WNP D20 is in good agreement with the *in-situ* D20. However, moving northward to the IERZ [Fig. 4(c)], clear increase in spreading is found. In particular, the spreading is found to be caused by overestimation in the positive SSHA pairs (red circles) and underestimation in the negative SSHA pairs (blue squares). Further north to the NERZ [Fig. 4(d)], a huge error is seen. One can see that the derived D20 can reach 300 m in the positive SSHA region, with an overestimation of ∼200 m from the *in-situ* D20 of ∼100 m [also in Fig. 6(a)], while underestimation in t he negative SSHA region is again observed.

TABLE II
APPLICABILITY OF THE DEPTH OF 20 °C ISOTHERM (D20) USING THE TLM_WNP METHOD FOR DIFFERENT MONTHS AND ZONES. USING THE 25% PROM AS THE ACCEPTANCE THRESHOLD, THE "APPLICABLE" MONTHS AND ZONES ARE SHOWN BY TICKS, WHILE THE OTHER MONTHS AND ZONES ARE SHOWN BY CROSSES

	May	June	July	August	September	October
NERZ	×	×	×	×	×	×
IERZ	×	×	×	×	×	×
SERZ	√	√	√	√	√	√
SNPG	√	√	√	√	√	√

From the accuracy analysis in Fig. 5, we can see that, in the SNPG and SERZ, the rms difference is usually about 25 m or less, bias < 20 m, and PROM $< 25\%$. However, in the IERZ, the bias increases to > 25 m, and the PROM reaches ∼30%. As in the NERZ, both rms difference and bias can be as much as 100 m, while the PROM can also reach 100%. Taking a PROM of 25% as a threshold guide, the applicable regions/months are determined and summarized in Table II. Basically, the two-layer-method-derived D20 is of acceptable accuracy in the SNPG and SERZ but not in the IERZ and, particularly, NERZ. Possible reasons for these inapplicabilities are discussed as follows: From Fig. 6, one can see that the hydrographic setting in the NERZ and IERZ is complex. There exists a mixed-water region where the warm Kuroshio current from the south and the cold Oyashio current from the north mixed, a cold sub-Arctic current, and a recirculation region in the Kuroshio extension [28]. With this complex situation, the simple two-layer method may not work. Another possibility is the assumption that is made in choosing D20 as the border separating the two layers (Section II). D20 was chosen and proposed originally as it is usually where the main thermocline in the study region of Shay *et al.* [32], i.e., the Gulf of Mexico, lies. In [10], this method and the choice of D20 are subsequently applied globally. It is possible that, in the IERZ and NERZ, D20 may not be an appropriate choice in representing the thermocline location and resulted in the observed error in estimation. As reported by Qui and Chen [29], in these regions, the main thermocline is below 20 °C and can reach as low as 12 °C, suggesting possible errors of using D20 in these regions. This can be tested in future investigations and assess whether accuracy can be improved by changing the choice of D20 in the IERZ and NERZ.

B. Validation of the Depth of the 26 °C Isotherm (D26) and SST

After estimating D20, D26 can then be estimated from (2) (Section II) based on the estimated D20. According to the validation results of D20 (Section III-A), the two-layer method cannot produce reliable D20 in the IERZ and NERZ. Thus, in these two zones, D26 is not calculated. As in Fig. 7(a), it can be seen in the monthly scatter plots that the derived and observed D26 in the SNPG is again in good agreement for all the months between May and October. The corresponding rms difference is typically about 12 m with bias < 3 m and a PROM of about 12% (Fig. 8). In the SERZ, a similar agreement is

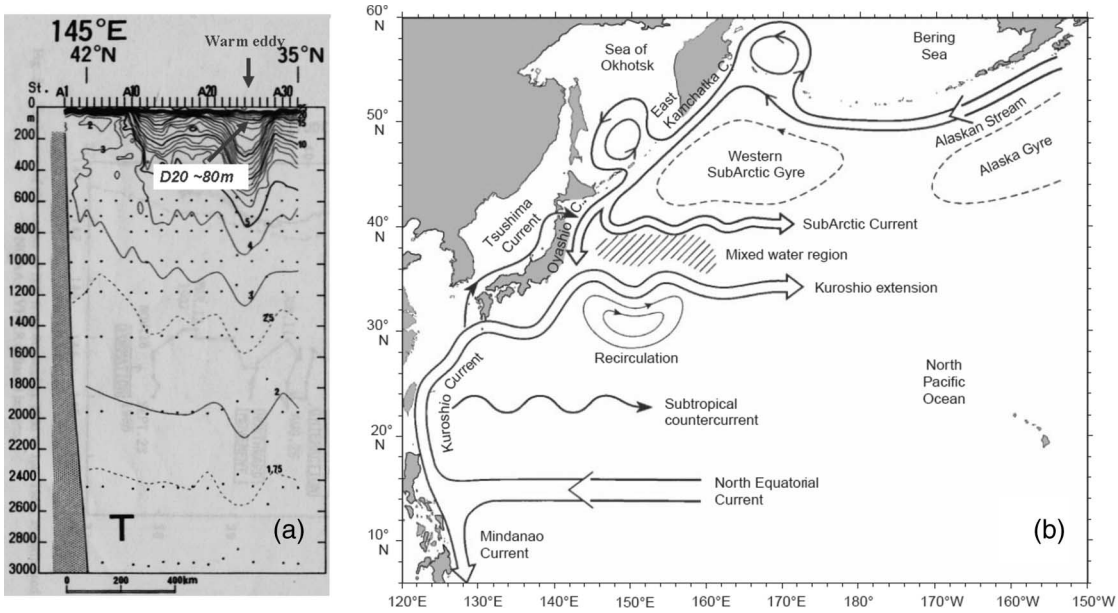

Fig. 6. (a) Observational temperature transect of 145° E in the NERZ (after [37]). (b) Hydrographical setting of the western North Pacific (after [28]).

found from July to October [Figs. 7(b) and 8]. In May and June, clear underestimation in the positive SSHA pairs (red circles) is seen [Fig. 7(b)]. This leads to a decrease in the accuracy that the rms difference is about 22–25 m and the PROM is about 32%–38%. This shows unreliable estimation of D26 in these two months. This inapplicability of the two-layer method in the SERZ during the early typhoon season (e.g., May and June) may be caused by the uncertainty of θ (i.e., the climatological ratio between D20 and D26). As shown in Fig. 2(a), during these months, θ is of very low value (0–0.3) and shoals sharply in the SERZ (122–170° E, 18–25° N) during this early period before summer. With this very low and sharp decrease in θ, D26 can be underestimated as observed. Table III summarizes the applicable months in the SNPG and SERZ of the D26 estimation. The validation results of SST are given in Fig. 9. One can see that the monthly rms difference between the TLM_WNP (i.e., the TRMM/TMI and AMSR-E SST) and the observed GTSPP SST is within the range of 0.4 °C–1 °C. The bias is typically below 0.5 °C, showing good agreements. A similar finding was also reported by [36].

C. Applicable Zones and Periods

As summarized in Tables II and III, the two-layer method is applicable in the southern part of the western North Pacific ocean (i.e., the SNPG and SERZ) but not in the northern part (i.e., IERZ and NERZ). Thus, SNPG and SERZ are the "applicable" zones where this method can be used with acceptable accuracy (typically, the monthly PROM is $< 25\%$). In addition, the applicable months of the SNPG are from May to October (i.e., the entire typhoon season), while those of the SERZ are from July to October. To assess whether this limited applicability in location and time may pose a serious constraint in studying typhoon intensification, we analyze 45 years (1960–2004) of typhoon track and intensity data over the western North Pacific during the May–October period. The data source of this analysis is the best track data of the U.S. Joint Typhoon Warning Center (JTWC). Table IV compares the number of typhoons (during intensification) passing the applicable zones during the applicable months with the total (i.e., passing both inside and outside of the applicable zones and months). As shown in Table IV, this limited applicability should not pose a severe constraint in studying the intensification of category 5 (in Saffir–Simpson scale) typhoons since 100% of category 5 typhoons are found to intensify only in the applicable zones [21]. One can also see that 96.2% of category 4 intensifying typhoons and 97% of category 3 typhoons pass the applicable zones and applicable months. This suggests that, although TLM_WNP is only applicable in the applicable zones during applicable months, this limited applicability is not a severe hindrance when studying the intensification of intense (i.e., categories 3–5) typhoons since most (96.2%–100%) of these intense typhoons are found to intensify in the applicable zones during applicable months. The limited applicability of the two-layer method for category 2 and, particularly, category 1 typhoons, however, poses some constraints. As shown in Table IV, 61.9% of the category 1 typhoons pass the applicable zones during applicable months during their intensification, while the other 38.1% of the category 1 typhoons do not. As for category 2, 87.9% of the cases are applicable. Fig. 10 summarizes the intensification track segment for all 562 typhoons (from category 1 to 5) passing the western North Pacific and, in average, 84.5% of the typhoons that are intensified in the applicable zones during applicable months (as also shown in Table IV).

IV. Comparison With the NPACNFS Full Ocean Model

Since the two-layer reduced-gravity model is a simple model, here we further compare its performance with the NPACNFS full ocean model from the U.S. NRL [18]. NPACNFS is a 3-D

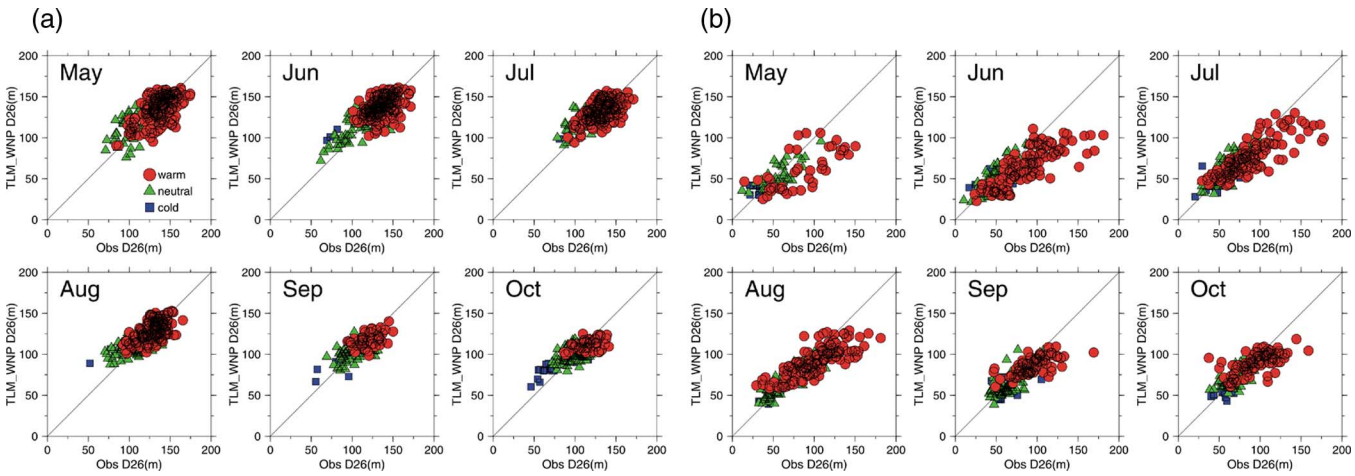

Fig. 7. As in Fig. 4, the monthly scatter plots of the TLM_WNP-estimated D26 and the *in-situ* GTSPP D26 in the (a) SNPG and (b) SERZ during 2002–2005.

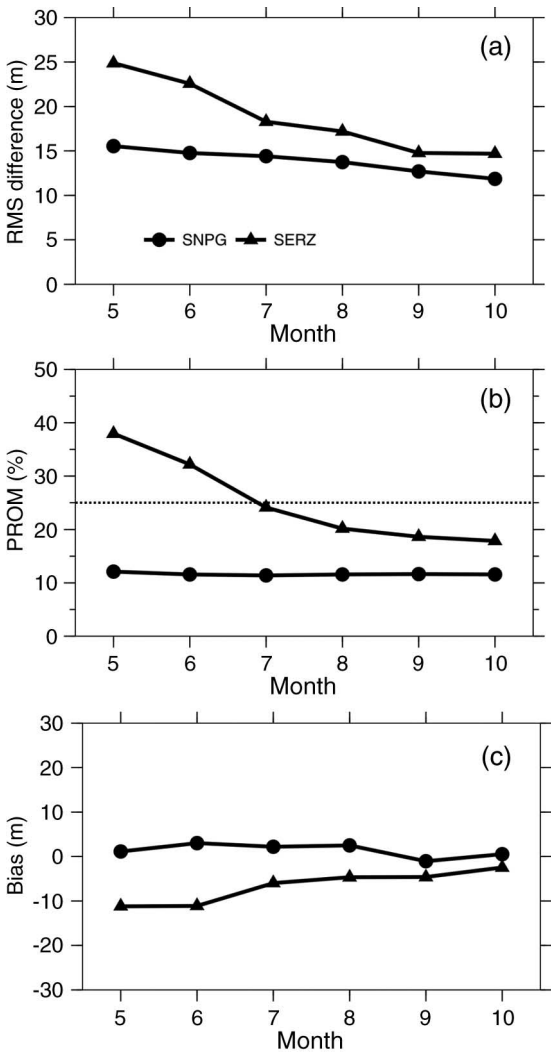

Fig. 8. (a) Monthly rms difference, (b) PROM, and (c) bias of the TLM_WNP-estimated D26 in SNPG and SERZ. The dotted line in (b) depicts the accuracy threshold of 25% PROM.

TABLE III
AS IN TABLE II BUT FOR THE 26 °C ISOTHERM (D26) THAT IS ESTIMATED USING THE TLM_WNP

	May	June	July	August	September	October
NERZ	×	×	×	×	×	×
IERZ	×	×	×	×	×	×
SERZ	×	×	√	√	√	√
SNPG	√	√	√	√	√	√

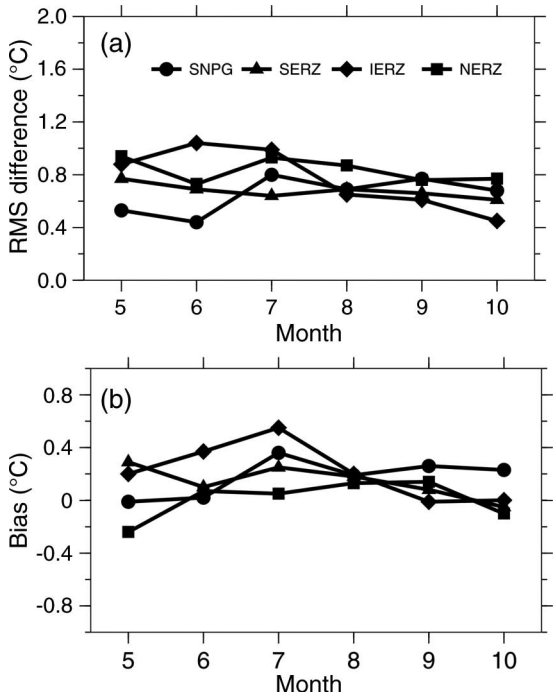

Fig. 9. Comparison of the value of (a) rms difference and (b) bias for the SST in the TLM_WNP in the SNPG, SERZ, IERZ, and NERZ.

hydrodynamic model with 26 sigma levels in the vertical. The model assimilated satellite data, MultiChannel SST (MCSST), and static climatology from the Modular Ocean Data Assimilation System to produce 3-D fields of temperature and salinity [18]. Three months (July–September 2003) of the NPACNFS upper ocean thermal structure data is obtained for comparison. Again, the NPACNFS data is validated by the *in-situ* GTSPP data.

TABLE IV
STATISTICS OF 45 YEARS (1960–2004) OF WESTERN NORTH PACIFIC TYPHOONS (CATEGORY 1 THROUGH 5) BASED ON THE BEST TRACK DATA FROM THE JOINT TYPHOON WARNING CENTER. THE TOTAL NUMBERS OF TYPHOONS (DURING INTENSIFICATION) ARE COMPARED WITH THE NUMBERS OF TYPHOONS PASSING THE APPLICABLE ZONES DURING APPLICABLE MONTHS

	Cat 1	Cat 2	Cat 3	Cat 4	Cat 5	Total
Total typhoon numbers	139	99	97	133	94	562
Passing applicable areas	86	87	80	128	94	475
Percentage	61.9%	87.9%	97%	96.2%	100%	84.5%

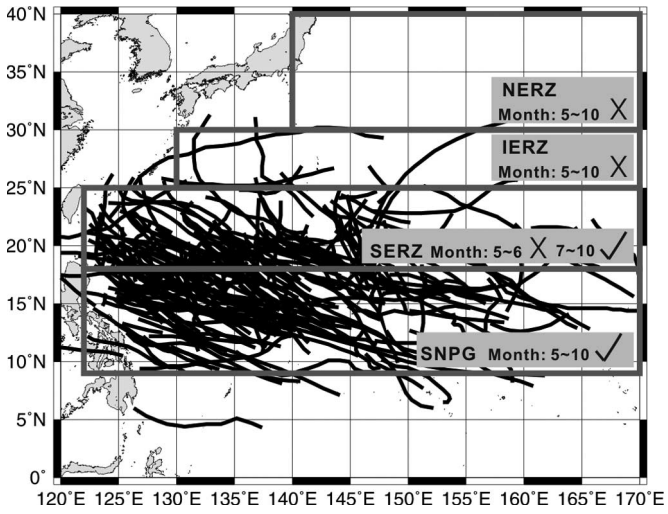

Fig. 10. Tracks of the 562 typhoons in the past 45 years (1960–2004) passing the western North Pacific and the applicable areas.

A. Depth of the 20 °C Isotherm (D20)

The validation results of the NPACNFS D20 are shown in Fig. 11(a)–(c). It can be seen that, during the three months of the validation period, the NPACNFS D20 shows slight increase in accuracy in the SNPG as compared with the two-layer method (Fig. 5) that the monthly rms difference is typically about 13–20 m with a PROM $< 10\%$. A small negative bias of about 10 m in the SNPG between July and September is noted. In the SERZ, the NPACNFS and TLM_WNP have similar accuracies in the D20 estimation, with a PROM of about 11%–16% and an rms difference of about 21 m in August and September [Fig. 11(a) and (b)]. A larger monthly rms difference of 32 m is noted in the NPACNFS D20 in July [Fig. 11(a)]. In the IERZ, the D20 from the NPACNFS performs better than that from the two-layer method (Fig. 5); for example, in July and September, the PROM is $< 20\%$ (rms difference < 20 m), while in August, the PROM is $\sim$29% [Fig. 11(a) and (b)]. In the NERZ, the D20 from the NPACNFS is better than that from the two-layer method, with a monthly PROM in the range of 43%–56% and an rms difference of about 30–46 m [Fig. 11(a) and (b)], as compared with the two-layer PROM of $> 90\%$ and rms difference of 70 m. However, although NPACNFS behaves better than the two-layer method in the NERZ, the rms of $\sim$40 m and PROM of $\sim$50%, as validated by the *in-situ* points, are still too high and are still not suitable for use. A summary of the applicability for applicable zones and months using the NPACNFS is given in Table V.

B. Depth of the 26 °C Isotherm (D26) and SST

The validation results of the NPACNFS D26 are summarized in Fig. 11(d)–(f). In comparison with the two-layer method (Fig. 8), the NPACNFS D26 has little less accuracy in the SNPG that the monthly PROM is $> 14\%$, as compared with the 11% of the two-layer method. In addition, a clear negative bias in the range of 8%–23% is found. In the SERZ, the two-layer D26 has higher accuracy that the PROM of the NPACNFS D26 can be up to 46% [Fig. 11(e)], while the two-layer PROM is about 20% [Fig. 8(b)]. Moving northward to the IERZ and NERZ, an obvious negative bias of the NPACNFS D26 with PROM $> 40\%$ is found, again suggesting that in these two zones, even with the complex NPACNFS, D26 cannot be reliably estimated. Again, taking the 25% monthly PROM accuracy as a threshold, the applicability of the NPACNFS is summarized in Table VI.

The validation results of the NPACNFS SST with *in-situ* data are given in Fig. 11(g) and (h). In contrast to the high SST accuracy that is found in the two-layer method (i.e., monthly rms difference and bias ~ 0.7 °C), the NPACNFS shows less accuracy. As shown in Fig. 11(g) and (h), the monthly rms difference is in the range of 0.8 °C–1.4 °C, together with a clear negative bias of 1.0 °C. From the preceding discussion, we see that the NPACNFS has general underestimation in the upper ocean parameters (i.e., D26 and SST). This becomes a critical factor to consider when using NPACNFS upper ocean parameters to study typhoon–ocean interaction since this upper ocean is the primary part of the ocean with which typhoons are interacting [25], [32].

Fig. 12 compares the profiles from the *in-situ*, two-layer, and NPACNFS profiles along a transect at 145° E for every 3° latitude from 10° N to 25° N (i.e., passing through SNPG and SERZ). Here, the 145° E transect is chosen because it is where abundant *in-situ* profiles exist with uniform distribution (Fig. 3). In Fig. 12, one can see that the simple two-layer profiles (in gray with dots) match reasonably well with the observed profiles (black curves), while the clear underestimation (1.0 °C or more) of the upper ocean (typically from SST down to a depth of 100 m) of the NPACNFS profiles is seen.

C. TCHP

Using *in-situ* profiles, TCHP is calculated and used to compare with the TCHP from the estimated profiles by the two-layer and the NPACNFS models. From Fig. 13, one can see that the two-layer TCHP has higher accuracy than the NPACNFS TCHP throughout the three-month (July–September 2003) validation period. With the two-layer method, the rms difference is about 30 kJ/cm^2, and the bias is less than 10 kJ/cm^2. In contrast, the NPACNFS TCHP has evident underestimation with a large negative bias ranging from -40 to -60 kJ/cm^2 and the large corresponding PROM in the range of 40%–70% (Fig. 13). This

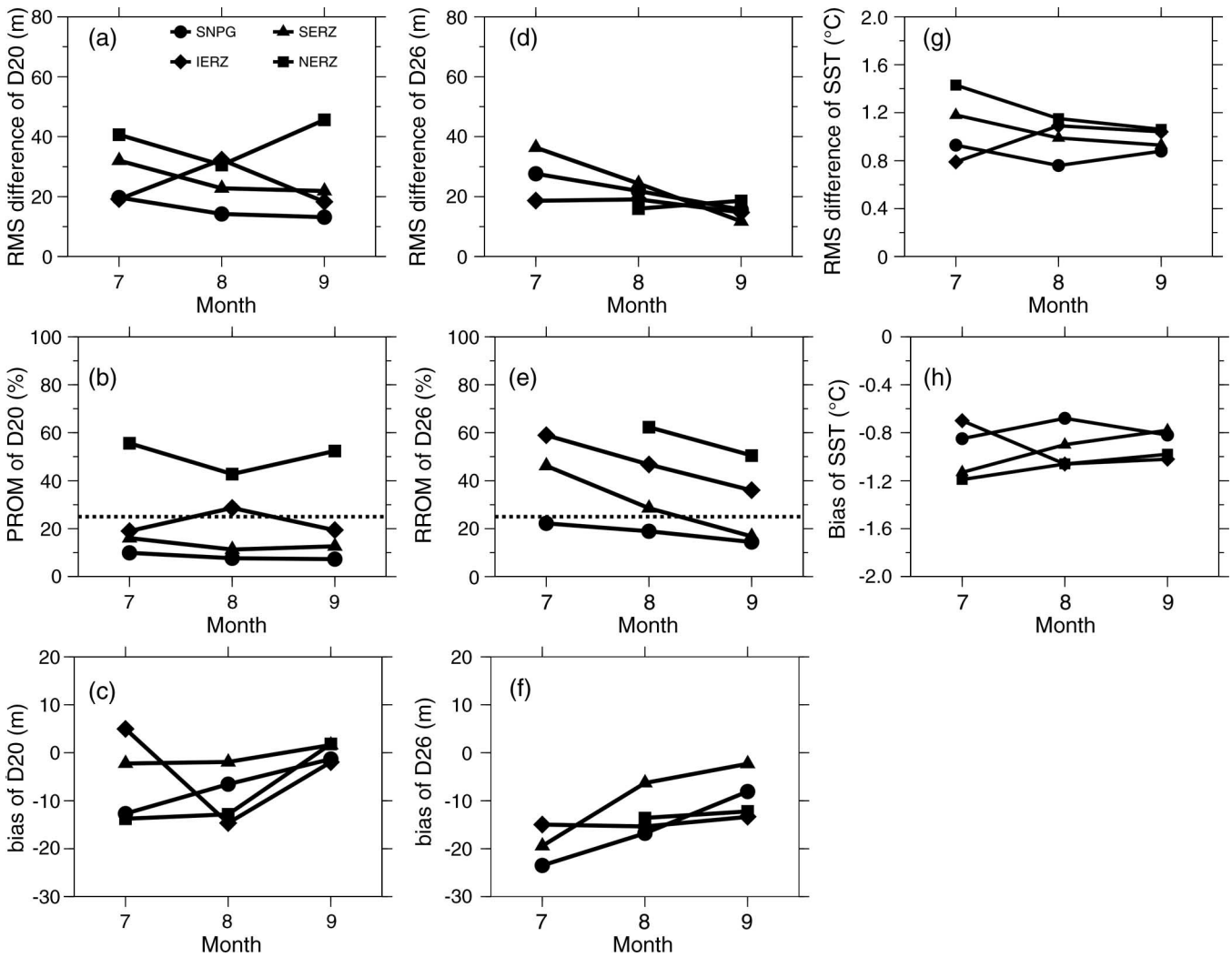

Fig. 11. Comparison of the value of the monthly rms difference, PROM, and bias of the NPACNFS profiles for (a)–(c) D20, (d)–(f) D26, and (g) and (h) SST. The dotted line in (b) and (e) depicts the accuracy threshold of the 25% PROM.

TABLE V
AS IN TABLE II BUT FOR THE PERFORMANCE OF THE NPACNFS D20

	August	September	October
NERZ	×	×	×
IERZ	√	×	√
SERZ	√	√	√
SNPG	√	√	√

TABLE VI
AS IN TABLE II BUT FOR THE PERFORMANCE OF THE NPACNFS D26

	August	September	October
NERZ	×	×	×
IERZ	×	×	×
SERZ	×	×	√
SNPG	√	√	√

underestimation is clearly the result of the underestimation of SST and D26 in the NPACNFS profiles, as discussed in Section IV-B.

V. APPLICATION IN STUDYING THE INTENSITY CHANGE OF SUPERTYPHOON DIANMU (2004)

Using the TLM_WNP profiles, we study the intensity change of Supertyphoon Dianmu (2004). Dianmu, which means "Mother of lighting" in Chinese and made landfall and damaged Japan, has been the most rapidly intensified western North Pacific typhoon since 1960.[2] Within 18 h (0000 UTC–1800 UTC June 15), it rapidly intensified from category 1 (70 kn) to the category 5 superscale (145 kn). This is equivalent to 100-kn intensification in 24 h, which is more than three times the usual "rapid intensification" baseline of 30 kn in 24 h [15]. Observing the pre-Dianmu SSHA data, one can see that this happened as Dianmu entered a large warm ocean feature region in the SNPG that is characterized by positive SSHA $\sim$20 cm [Fig. 14(a)]. From the TLM_WNP results, we can see that this warm feature caused further deepening of D26 by 10–30 m [Fig. 14(b)] in the SNPG. As a result, it can be

[2]According to the 1-min sustained wind best track data of the U.S. JTWC from 1960 to present, Dianmu (2004) and the #11 typhoon in 1983 are the most rapidly intensified typhoons in the western North Pacific; both intensified by 75 kn within 18 h.

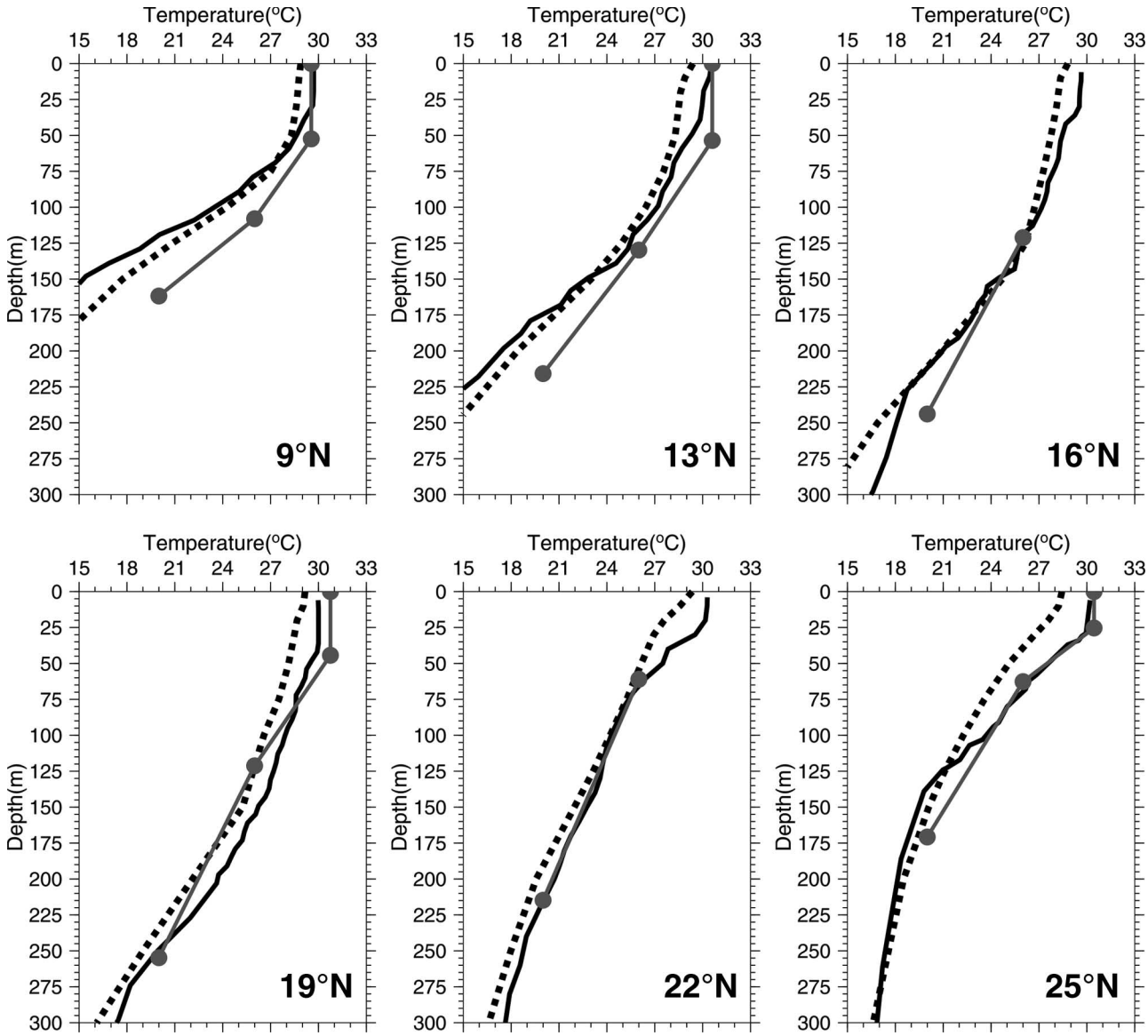

Fig. 12. Comparison of the (black) *in-situ*, (gray with dots) TLM_WNP, and (dotted curve) NPACNFS profiles in the SNPG and SERZ. Along the transect of 145° E from 10–25° N, the profiles for every 3° interval are compared. In the 13° N and 19° N TLM_WNP profiles, the SST data are not available.

seen that this rapid intensification took place at a region with an extraordinarily thick layer of warm water, i.e., D26 reaching 150 m [Fig. 14(c)]. The corresponding pretyphoon TCHP is about 120–150 kJ/cm^2 [Fig. 14(d)], which is higher than the well-known Hurricane Opal (1998) case of 80–120 kJ/cm^2 [10], [32]. As it progressed into the interior of the warm feature at 0600 UTC June 16, Dianmu reached its peak intensity at 155 kn [Fig. 14(a) and (c)]. This peak intensity sustained for 12 h until 1800 UTC June 16 and started to decline to the category 4 120 kn at 1800 UTC June 17 as Dianmu moved into a region with a shallower warm layer of 90 m [Fig. 14(c)]. This situation can also be seen from the TLM_WNP profiles, where profiles from the intensification region (i.e., profiles 1–6), the intensity-sustained region (profiles 7 and 8), and the intensity declination region (profiles 9–12) are depicted in red, green, and blue, respectively [Fig. 15(a)]. Here, two *in-situ* GTSPP profiles (profile 6′ and 9′) that were found prior to Dianmu's passing (from June 10 and 12, 2004; one near profile 6 and one near profile 9) are depicted in black (Fig. 15(a), with the location depicted as stars in Fig. 14), confirming acceptable quality of the TLM_WNP profiles. It can also be noted that, with the two-layer method, profiles along the track can be obtained, but with *in-situ* profiles, such information is not available. As in the Dianmu case, only two *in-situ* profiles are found. As reported by Lin *et al.* [21], this lacking of *in-situ* data along the typhoon's tracks is common, particularly, before the deployment of Argo floats [11], [12] in 2003.

Thus, with the TLM_WNP profiles as initialization, together with wind forcing from the JTWC best track wind, we can run an ocean mixed-layer model [26] to study the ocean's dynamic response to typhoon and estimate typhoon-induced cooling [1], [3], [25]. From Fig. 15(b), one can see the progressive increase in mixing as the typhoon intensifies (profiles 1–6) and reaching as deep as 120 m, as confirmed by the *in-situ* GTSPP profile [black profile in Fig. 15(b), with the location depicted as a triangle in Fig. 14] that was acquired immediately after the

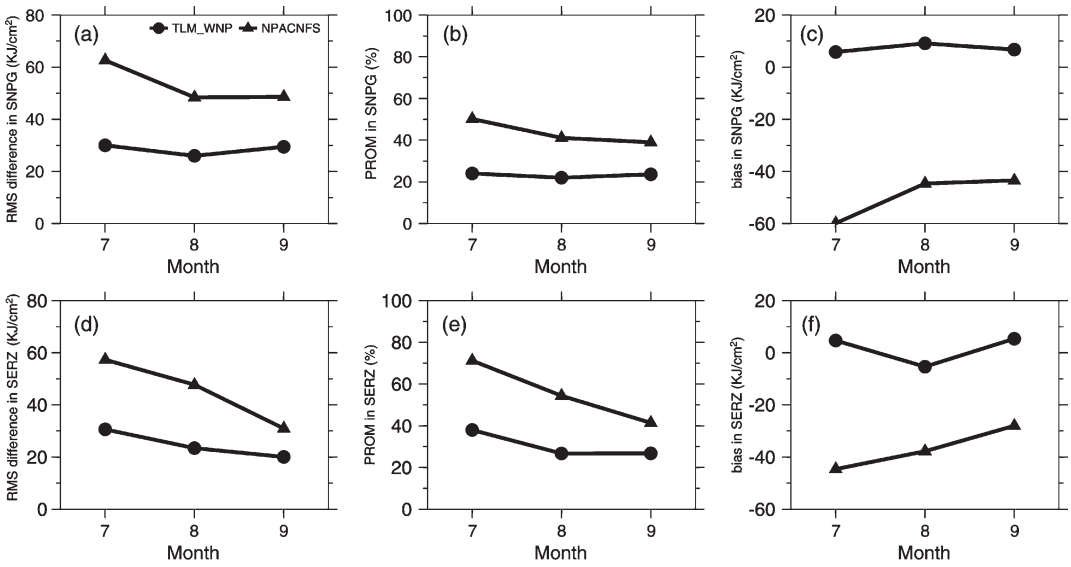

Fig. 13. Comparison of the value of the monthly rms difference, PROM, and bias for the TCHP estimation using the TLM_WNP and the NPACNFS profiles for (a)–(c) SNPG and (d)–(f) SERZ.

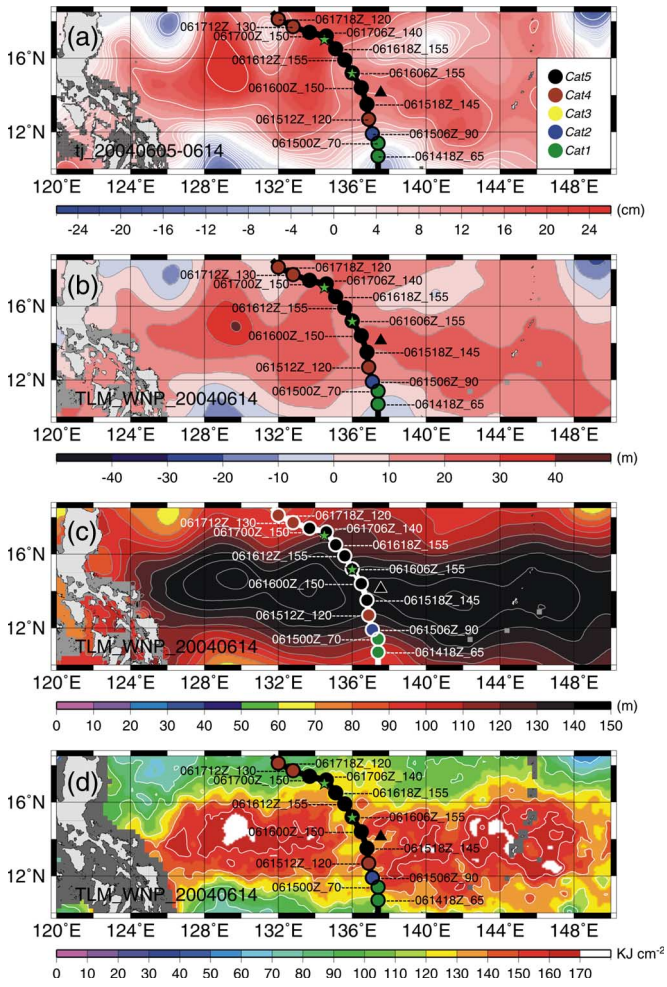

Fig. 14. (a) Composite of TOPEX/Poseidon and Jason-1 altimetry measurements for one cycle (ten days) between June 5, 2004 and June 14, 2004, showing the pre-Dianmu SSHA. (b) ΔD26 (TLM_WNP-derived D26 minus climatological D26), (c) TLM_WNP-derived D26, and (d) TCHP estimated from the two-layer method. The green stars and black triangle depict the *in-situ* profiles that are found before and during Dianmu's passage. Typhoon intensity in the Saffir–Simpson scale is shown in the legend of (a).

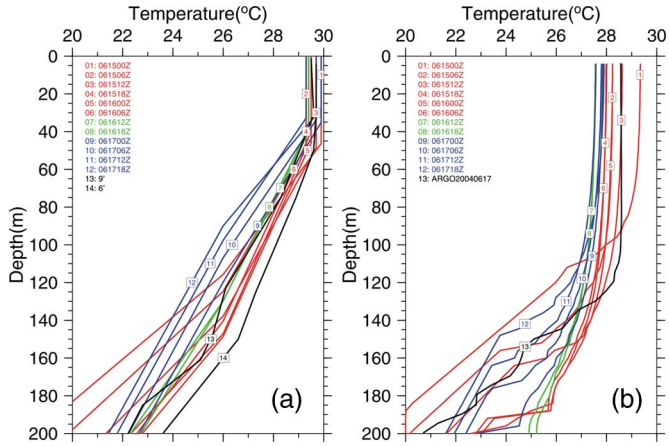

Fig. 15. (a) Initial profiles along Dianmu's track that are used in the mixed-layer model experiment where the *in-situ* profiles, those along Dianmu's intensification location, those along Dianmu's intensity maintenance location, and those along Dianmu's intensity decay location are depicted in black, red, green, and blue, respectively. (b) same as (a), but from mixed-layer model except profile 13, which obtained from ARGO.

intensification period on June 17, 2004. From Fig. 16, one can also see the corresponding increase in self-induced cooling from 0.6 °C during category 1 (at 0000 UTC June 15) to 1.4 °C at peak (i.e., category 5, 0600 UTC June 16). From 0600 UTC June 16 onward, although Dianmu's intensity did not increase, cooling still enhanced to 2.1 °C as Dianmu moved into a region with shallower warm water [profiles 9–12 in Fig. 15(b), Fig. 16]. This situation can also be observed in the SST maps from TRMM and AMSR-E that were acquired before [on June 13, Fig. 17(a)] and after [on June 18, Fig. 17(b)] Dianmu's passing. From 0600 UTC June 16 onward, one can see clear enhanced cooling to the right to the typhoon's track [SST $\sim$ 27 °C in Fig. 17(b)] [1], [2], [25], [36] as compared with the warm pretyphoon SST of $>$ 29 °C [Fig. 17(a)]. As in the earlier intensification period (i.e., before 0600 UTC June 16), cooling is less pronounced [Fig. 17(b)].

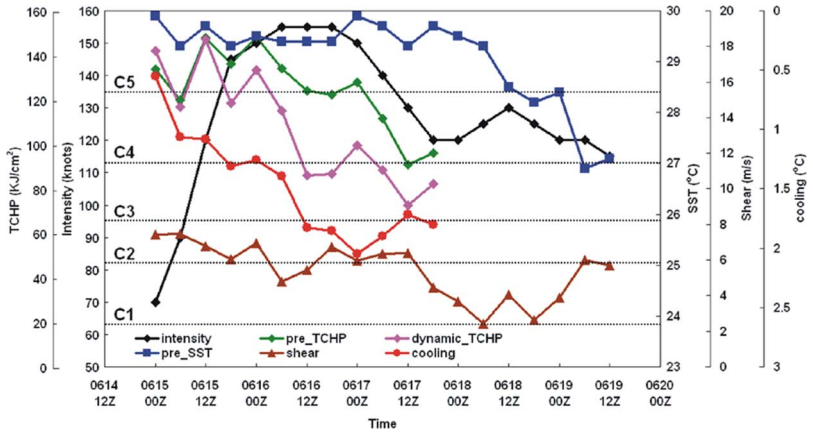

Fig. 16. Relationship between five parameters (i.e., self-induced SST cooling, dynamic TCHP, pretyphoon SST, pretyphoon TCHP, and vertical wind shear) and typhoon intensity.

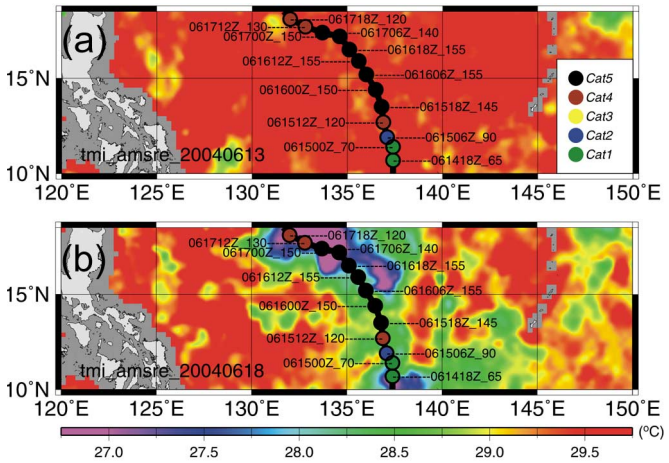

Fig. 17. Composite of SST from the TMI and AMSR-E passes in (a) June 13, 2004 for pre-Dianmu and in (b) June 18, 2004 for after Dianmu's passage.

Finally, of much interest for future forecast reference is to identify parameters that are sensitive to typhoon-intensity change. As shown previously, using the derived profiles to the mixed-layer model, self-induced cooling during the typhoon along the track can be estimated. Since upper ocean thermal profiles [i.e., Fig. 15(b)] can also be obtained, it can be used to calculate the dynamic TCHP during the typhoon. Therefore, two parameters that include the ocean's dynamic response, i.e., the self-induced cooling and the dynamic TCHP during the typhoon, can be calculated. It should be noted that, without the derived profiles, these two parameters could not be calculated, as it is impossible to have *in-situ* profiles at each point of the track (Fig. 14). Together with the other parameters, i.e., pretyphoon SST [blue curve in Fig. 16 and the 2-D map in Fig. 17(a)], pretyphoon TCHP [green curve in Fig. 16, as from Fig. 14(d)], and atmospheric vertical wind shear[3] data along the track (brown curve in Fig. 16), we compare the sensitivity of these five parameters to typhoon-intensity change during Dianmu's drastic intensity change period (i.e., covering the rapid-intensification period from category 1 to 5, followed by the decay to category 4, from 0000 UTC June 15 to 1800 UTC June 17). From Fig. 16, we can see that throughout the study period, there is little change in the vertical wind shear. With the rapid intensification and decay of Dianmu, the shear was typically about 6 m/s and shows little variability. This is also true for the pretyphoon SST. In comparison, the other three parameters, i.e., the pretyphoon TCHP, the dynamic TCHP, and the self-induced cooling, have more variability. As can also be seen in the relationship between the 6-h intensity change and each of the five parameters (Fig. 18), the two parameters that include the ocean's dynamic responses, i.e., the self-induced cooling and the dynamic TCHP, have the highest correlation coefficient, with $R^2 = 0.69$ and 0.72, respectively [Fig. 18(a) and (b)]. This suggests that there seems to be a relation between the 6-h intensity change of Dianmu during this period and these two parameters. During this study period, the correlation coefficient with the pretyphoon SST and the vertical wind shear is low, with $R^2 = 0.07$ and 0.10, respectively [Fig. 18(c) and (e)]. As for the pretyphoon TCHP, $R^2 = 0.48$ shows more sensitivity than the pretyphoon SST and shear but is still lower than the self-induced cooling and the dynamic TCHP.

It should be understood that typhoon intensity is controlled by many necessary atmospheric and oceanic parameters as well as the typhoon's own structure [4], [35]. It is still a current open question in identifying sensitive parameters in typhoon intensity and identifying the roles that each parameter plays [4], [5], [10], [35]. The preceding sensitivity comparison shows that pretyphoon SST and vertical wind shear are less sensitive than the other parameters. However, it does not imply that both parameters are not important. The very warm pretyphoon SST in the range of 29 °C–30 °C and the low wind shear of about 6 m/s [8] are all very favorable for typhoon intensification but not sensitive to subsequent typhoon-intensity change when the value of the threshold of both parameters (i.e., pretyphoon SST > 26 °C and wind shear < 10 m/s) are satisfactory. Unless the situation is close to threshold value, both parameters can probably become sensitive to typhoon intensity. In the Dianmu's case, both parameters were far beyond the threshold and experienced little change (blue and brown curves

[3]Wind shear is estimated as the difference between the 200- and 850-mb European Centre for Medium-Range Weather Forecasts 1.25° resolution reanalysis wind data that are averaged over a 700 × 700 km box that is centered in the typhoon for every 6-h interval.

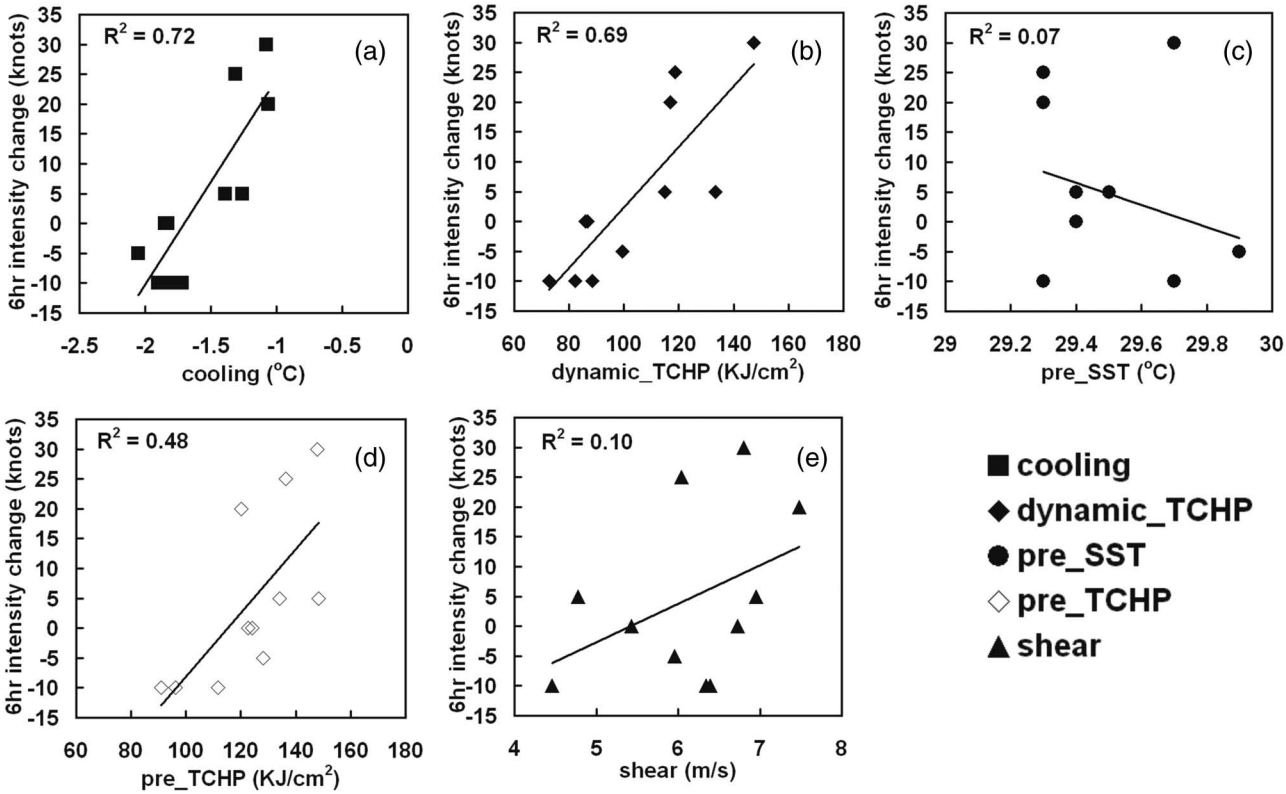

Fig. 18. Intensity change of 6 h of Dianmu with the five parameters, i.e., (a) self-induced SST cooling, (b) dynamic TCHP, (c) pretyphoon SST, (d) pretyphoon TCHP, and (e) vertical wind shear.

in Fig. 16) during the study period; thus, pretyphoon SST and vertical wind shear are not as sensitive as the other parameters. This study is the beginning of investigation using two-layer-method-derived profiles to systematically study these various parameters in relation to the intensity change of western North Pacific typhoons. With the current analysis, we found that at least for the Dianmu case, the upper ocean thermal structure is highly critical, and the two associated parameters, i.e., the self-induced cooling and the dynamic TCHP during typhoon, are the most sensitive to the 6-h intensity change as compared with all other parameters.

VI. Conclusion

Using a large set of $>$ 5000 *in-situ* profiles from the NOAA/GTSPP database during 2002–2005, this paper validates the upper ocean thermal structure data that are derived from using satellite altimetry and SST in a two-layer reduced-gravity ocean model that was proposed by Goni *et al.* [9] and Shay *et al.* [32] for the western North Pacific ocean. The validation period is during the May–October typhoon season from 2002 to 2005. After validation, applicable zones and months where this method can apply are identified. We found that the two-layer method is applicable in the southern and central western North Pacific (i.e., 122–170° E, 18–25° N) during most of the typhoon months. However, it is not applicable in the northern part (i.e., 130–170 °E, 25–40° N). Further comparison with the NRL's NPACNFS 26-level hydrodynamic model shows that the NPACFNS also experiences a similar regional dependence. In addition, clear underestimation in the upper ocean parameters (i.e., SST and D26) is found. This leads to significant underestimation in TCHP using the NPACNFS profiles from -40 to -60 kJ/cm^2, whereas using the two-layer method, the TCHP estimation reaches higher accuracy, which is typically about 30 kJ/cm^2. Applying the two-layer-method-derived profiles in studying the intensity change of supertyphoon Dianmu (2004) found that the two parameters, i.e., the typhoon's self-induced cooling and the dynamic TCHP during the typhoon, are the most sensitive parameters $(R^2 \sim 0.7)$ to the 6-h intensity change during the study period. Therefore, with the availability of the upper ocean thermal profile that is derived from the two-layer method in the applicable zones/periods in the western North Pacific, one can conduct future analysis to systematically study the control of upper ocean thermal structure in the intensity change of western Pacific typhoons.

Acknowledgment

The authors would like to thank the reviewers for their very thorough review and helpful suggestions and the NOAA/NODC, the NASA/Jet Propulsion Laboratory, and the Remote Sensing Systems for data provision.

References

[1] M. A. Bender and I. Ginis, "Real-case simulations of hurricane–ocean interaction using a high-resolution coupled model: Effects on hurricane intensity," *Mon. Weather Rev.*, vol. 128, no. 4, pp. 917–946, 2000.

[2] S. W. Chang and R. A. Anthes, "The mutual response of the tropical cyclone and the ocean," *J. Phys. Oceanogr.*, vol. 9, no. 1, pp. 128–135, Jan. 1979.

[3] K. A. Emanuel, "Thermodynamic control of hurricane intensity," *Nature*, vol. 401, no. 6754, pp. 665–669, Oct. 1999.

[4] K. A. Emanuel, C. DesAutels, C. Holloway, and R. Korty, "Environmental control of tropical cyclone intensity," *J. Atmos. Sci.*, vol. 61, no. 7, pp. 843–858, Apr. 2004.
[5] K. A. Emanuel, "Increasing destructiveness of tropical cyclones over the past 30 years," *Nature*, vol. 436, no. 7051, pp. 686–688, Aug. 2005.
[6] M. DeMaria and J. Kaplan, "Sea surface temperature and the maximum intensity of Atlantic tropical cyclones," *J. Climate*, vol. 7, no. 9, pp. 1324–1334, Sep. 1994.
[7] L. L. Fu, E. J. Christensen, C. A. Yamarone, M. Lefebvre, Y. Menard, M. Dorrer, and P. Escudier, "TOPEX/POSEIDON mission overview," *J. Geophys. Res.*, vol. 99, no. C12, pp. 24 369–24 381, 1994.
[8] G. M. Gallina and C. S. Velden, "Environmental wind shear and tropical cyclone intensity change using enhanced satellite derived wind information," in *Proc. Preprints, 25th Conf. Hurricanes and Tropical Meteorol.*, San Diego, CA, 2002, pp. 172–173.
[9] G. J. Goni, S. Kamholtz, S. Garzoli, and D. B. Olson, "Dynamics of the Brazil–Malvinas confluence based upon inverted echo sounders and altimetry," *J. Geophys. Res.*, vol. 101, no. 7, pp. 16 273–16 289, 1996.
[10] G. J. Goni and J. A. Trinanes, "Ocean thermal structure monitoring could aid in the intensity forecast of tropical cyclones," *EOS, Trans. Amer. Geophys. Union*, vol. 84, no. 51, pp. 573–580, 2003.
[11] J. Gould, D. Roemmich, S. Wijffels, H. Freeland, M. Ignaszewesky, X. Jianping, S. Pouliquen, Y. Desaubies, U. Send, K. Radhakrishnan, K. Takeuchi, K. Kim, M. Danchenkov, P. Sutton, B. King, B. Owens, and S. Riser, "Argo profiling floats bring new era of in situ ocean observations," *EOS, Trans. Amer. Geophys. Union*, vol. 85, no. 19, p. 179, 2004. 190–191.
[12] J. Gould, "From swallow floats to Argo—The development of neutrally buoyant floats," *Deep-Sea Res. II*, vol. 52, no. 3/4, pp. 529–543, 2005.
[13] X. Hong, S. W. Chang, S. Raman, L. K. Shay, and R. Hodur, "The interaction between Hurricane Opal (1995) and a warm core ring in the Gulf of Mexico," *Mon. Weather Rev.*, vol. 128, no. 5, pp. 1347–1365, May 2000.
[14] C. Hwang, C. R. Wu, and R. Kao, "TOPEX/Poseidon observations of mesoscale eddies over the subtropical countercurrent: Kinematic characteristics of an anticyclonic eddy and of a cyclonic eddy," *J. Geophys. Res.*, vol. 109, no. C8, p. C08013, 2004. DOI:10.1029/2003JC002026.
[15] J. Kaplan and M. DeMaria, "Large-scale characteristics of rapidly intensifying tropical cyclones in the North Atlantic basin," *Weather Forecast.*, vol. 18, no. 6, pp. 1093–1108, Dec. 2003.
[16] A. B. Kara, P. A. Rochford, and H. E. Hurlburt, "Naval research laboratory mixed layer depth (NMLD) climatologies," Stennis Space Center, Hancock, MS, NRL Rep. NRL/FR/7330-02-9995, 2002. 26.
[17] B. Keeley, C. Sun, and L. P. Villeon, "Global temperature and salinity profile program annual report," NOAA/National Oceanographic Data Center, Silver Spring, MD, 2003.
[18] D. S. Ko, R. H. Preller, G. A. Jacobs, T. Y. Tang, and S. F. Lin, "Transport reversals at Taiwan Strait during October and November 1999," *J. Geophys. Res.*, vol. 108, no. C11, p. 3370, 2003. 10.1029/2003JC001836.
[19] D. Leipper and D. Volgenau, "Hurricane heat potential of the Gulf of Mexico," *J. Phys. Oceanogr.*, vol. 2, no. 3, pp. 218–224, Jul. 1972.
[20] I-I Lin, C. C. Wu, K. A. Emanuel, I. H. Lee, C. R. Wu, and I. F. Pun, "The interaction of Supertyphoon Maemi (2003) with a warm ocean eddy," *Mon. Weather Rev.*, vol. 133, no. 9, pp. 2635–2649, 2005.
[21] I-I Lin, C. C. Wu, and I. F. Pun, "Supertyphoon boosters in the western North Pacific Ocean," *J. Atmos. Sci.*, 2006. submitted for publication.
[22] F. J. Millero, C. T. Chen, A. Bradshaw, and K. Schleicher, "A new high pressure equation of state for seawater," *Deep-Sea Res.*, vol. 27A, no. 3/4, pp. 255–264, 1980.
[23] E. Palmen, "On the formation and structure of tropical cyclones," *Geophysics*, vol. 3, pp. 26–38, 1948.
[24] N. Picot, K. Case, S. Desai, and P. Vincent, *AVISO and PODAAC User Handbook. IGRDR and GRD Jason Products*. France: CNES, 2003. SMM-MU-M5-OP-13184-CN (AVISO), JPL D-21352 (PODAAC), NASA, USA.
[25] J. F. Price, "Upper ocean response to a hurricane," *J. Phys. Oceanogr.*, vol. 11, no. 2, pp. 153–175, Feb. 1981.
[26] J. F. Price, R. A. Weller, and R. Pinkel, "Diurnal cycling: Observations and models of the upper ocean response to diurnal heating, cooling, and wind mixing," *J. Geophys. Res.*, vol. 91, no. C7, pp. 8411–8427, 1986.
[27] B. Qiu, "Seasonal eddy field modulation of the North Pacific Subtropical Countercurrent: TOPEX/Poseidon observations and theory," *J. Phys. Oceanogr.*, vol. 29, no. 10, pp. 1670–1685, Oct. 1999.
[28] B. Qiu, *Kuroshio and Oyashio Currents*. Honolulu, HI: Academic, Dept. Oceanogr., Univ. Hawaii at Manoa, 2001.
[29] B. Qiu and S. Chen, "Eddy-induced heat transport in the subtropical North Pacific from Argo, TMI and altimetry measurements," *J. Phys. Oceanogr.*, vol. 35, no. 4, pp. 458–473, Apr. 2005.
[30] D. Roemmich and J. Gilson, "Eddy transport of heat and thermocline waters in the North Pacific: A key to interannual/decadal climate variability?" *J. Phys. Oceanogr.*, vol. 31, no. 3, pp. 675–687, Mar. 2001.
[31] R. Scharroo, W. H. F. Smith, and J. L. Lillibridge, "Satellite altimetry and the intensification of hurricane Katrina," *EOS, Trans. Amer. Geophys. Union*, vol. 86, no. 40, pp. 366–367, Oct. 2005.
[32] L. K. Shay, G. J. Goni, and P. G. Black, "Effects of a warm oceanic feature on Hurricane Opal," *Mon. Weather Rev.*, vol. 128, no. 5, pp. 1366–1383, May 2000.
[33] C. Stephens, J. I. Antonov, T. P. Boyer, M. E. Conkright, R. A. Locarnini, T. D. O'Brien, and H. E. Garcia, "World Ocean Atlas 2001 Volume 1: Temperature," in *NOAA Atlas NESDIS 49*, S. Levitus, Ed. Washington, DC: U.S. GPO, 2002.
[34] UNESCO, "Algorithms for computation of fundamental properties of seawater," *Unesco Tech. Pap. Mar. Sci.*, no. 44, p. 53,1983.
[35] Y. Wang and C. C. Wu, "Current understanding of tropical cyclone structure and intensity changes—A review," *Meteorol. Atmos. Phys.*, vol. 87, no. 4, pp. 257–278, Dec. 2004.
[36] F. J. Wentz, C. Gentemann, D. Smith, and D. Chelton, "Satellite measurements of sea surface temperature through clouds," *Science*, vol. 288, no. 5467, pp. 847–850, May 2000.
[37] I. Yasuda, K. Okuda, and M. Hirai, "Evolution of a Kuroshio warm-core ring—Variability of the hydrographic structure," *Deep-Sea Res.*, vol. 39, no. 1, pp. 131–161, 1992.

Iam-Fei Pun received the B.S. degree in oceanography from National Taiwan Ocean University, Keelung, Taiwan, R.O.C., in 2002 and the M.S. degree in earth sciences from National Taiwan Normal University, Taipei, Taiwan, in 2005. He is currently working toward the Ph.D. degree at the Department of Atmospheric Sciences, National Taiwan University, Taipei.

He is developing a method for retrieving upper ocean thermal structures by satellite remote-sensing data and is studying its impact on typhoon intensity. His research interests include typhoon–ocean interaction and satellite remote sensing.

I-I Lin received the B.Sc. degree from the National Taiwan University, Taipei, Taiwan, R.O.C., in 1989 and the Ph.D. degree in remote sensing from the University of Cambridge, Cambridge, U.K., in 1995.

From 1995 to 1999, she was a Research Scientist in the Centre for Remote Imaging, Sensing, and Processing, National University of Singapore, Singapore. From 2000 to July 2004, she joined the National Center for Ocean Research, Taipei, as the Principal Investigator of the Remote Sensing Laboratory. In August 2004, she joined the Department of Atmospheric Sciences, National Taiwan University, as an Assistant Professor and, in 2006, as an Associate Professor. Her research interest include advanced multiple remote sensing to study air–sea physical and biogeochemical interaction related issues including typhoon–ocean interaction, dust storm–ocean interaction, and investigation the role of surfactants in air–sea gas exchange.

Chau-Ron Wu received the Ph.D. degree in physical oceanography from North Carolina State University, Raleigh, in 1998.

He is currently an Associate Professor with the Department of Earth Sciences, National Taiwan Normal University, Taipei, Taiwan, R.O.C. His research interests include coastal dynamics, satellite remote-sensing data analysis of oceanographic phenomena, numerical simulations on circulation models, and development of data assimilation techniques to integrate the measured data into numerical ocean models.

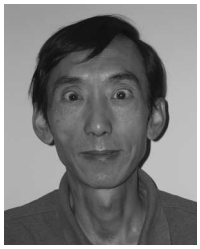

Dong-Shan Ko received the B.S. degree in marine science and the M.S. degree in physical oceanography from the College of Chinese Culture, Taipei, Taiwan, R.O.C., in 1974 and 1979, respectively, and the M.S. degree in ocean engineering and the Ph.D. degree in applied marine physics from the University of Miami, FL, in 1981 and 1987, respectively.

He is currently a Scientist in the Coastal and Semi-Enclosed Sea Section, Naval Research Laboratory (NRL), Stennis Space Center, MS. He has worked for a number of years on the development and design of ocean nowcast/forecast systems. He has also worked on applications of ocean models for the study of circulation in deep ocean basins and in the coastal ocean. His efforts at NRL were originally focused on the development of a forecast system along the west coast of USA and expanded to include the entire North Pacific Ocean. He is the Developer of NRL's real-time nowcast/forecast system in the Intra-Americas Sea and a Codeveloper of the real-time nowcast/forecast system in the East Asian Seas.

W. Timothy Liu received the Ph.D. degree in atmospheric sciences from the University of Washington, Seattle, in 1978.

In 1993, he became a Senior Research Scientist in the Jet Propulsion Laboratory (JPL), California Institute of Technology, Pasadena, which is equivalent to a Full Professor in major U.S. universities. From 1989 to 2005, he was the Leader of the Air–Sea Interaction and Climate Team at JPL. He is currently a Principal Scientist at JPL. He is the NASA Ocean Vector Wind Science Team Leader. He has been the Project Scientist of a series of NASA space missions, i.e., NSCAT, QuikSCAT, and SeaWinds. He was selected as Principle Investigator or a science team member of many Earth-observing space missions, including NSCAT, Topex/JASON, ERS-1, TRMM, EOS, Aqua, and AMSR. He has published 130 peer-reviewed scientific papers and book chapters. His research interests include ocean–atmosphere interaction and satellite oceanography.

Dr. Liu is a Fellow of the American Meteorological Society. He has chaired and participated in many science working groups and expert panels of NASA and the World Climate Research Program. He is the recipient of numerous scientific awards and medals from NASA and international organizations.